SCIENCE CHINA
Life Sciences

• RESEARCH PAPERS •

October 2011 Vol.54 No.10: 917–930
doi: 10.1007/s11427-011-4219-1

Mitogenomic analysis of the genus *Panthera*

WEI Lei[1,2], WU XiaoBing[1*], ZHU LiXin[3] & JIANG ZhiGang[4]

[1]*Anhui Provincial Key Laboratory of the Conservation and Exploitation of Biological Resources, College of Life Sciences, Anhui Normal University, Wuhu 241000, China;*
[2]*Faculty of Animal Science, Suzhou Vocational Technology College, Suzhou 234000, China;*
[3]*Department of Chemistry and Life Sciences, Chuzhou University, Chuzhou 239000, China;*
[4]*Laboratory of Animal Ecology and Conservation Biology, Institute of Zoology, Chinese Academy of Sciences, Beijing 100080, China*

Received January 5, 2011; accepted June 10, 2011

The complete sequences of the mitochondrial DNA genomes of *Panthera tigris*, *Panthera pardus*, and *Panthera uncia* were determined using the polymerase chain reaction method. The lengths of the complete mitochondrial DNA sequences of the three species were 16990, 16964, and 16773 bp, respectively. Each of the three mitochondrial DNA genomes included 13 protein-coding genes, 22 tRNA, two rRNA, one O_LR, and one control region. The structures of the genomes were highly similar to those of *Felis catus*, *Acinonyx jubatus*, and *Neofelis nebulosa.* The phylogenies of the genus *Panthera* were inferred from two combined mitochondrial sequence data sets and the complete mitochondrial genome sequences, by MP (maximum parsimony), ML (maximum likelihood), and Bayesian analysis. The results showed that *Panthera* was composed of *Panthera leo*, *P. uncia*, *P. pardus*, *Panthera onca*, *P. tigris*, and *N. nebulosa*, which was included as the most basal member. The phylogeny within *Panthera* genus was *N. nebulosa* (*P. tigris* (*P. onca* (*P. pardus*, (*P. leo*, *P. uncia*)))). The divergence times for *Panthera* genus were estimated based on the ML branch lengths and four well-established calibration points. The results showed that at about 11.3 MYA, the *Panthera* genus separated from other felid species and then evolved into the several species of the genus. In detail, *N. nebulosa* was estimated to be founded about 8.66 MYA, *P. tigris* about 6.55 MYA, *P. uncia* about 4.63 MYA, and *P. pardus* about 4.35 MYA. All these estimated times were older than those estimated from the fossil records. The divergence event, evolutionary process, speciation, and distribution pattern of *P. uncia*, a species endemic to the central Asia with core habitats on the Qinghai-Tibetan Plateau and surrounding highlands, mostly correlated with the geological tectonic events and intensive climate shifts that happened at 8, 3.6, 2.5, and 1.7 MYA on the plateau during the late Cenozoic period.

***Panthera uncia*, *Panthera pardus*, *Panthera tigris*, mtDNA, phylogeny, divergence time, Qinghai-Tibetan Plateau**

Citation: Wei L, Wu X B, Zhu L X, *et al*. Mitogenomic analysis of the genus *Panthera* . Sci China Life Sci, 2011, 54: 917−930, doi: 10.1007/s11427-011-4219-1

Living cat species (subfamily Felinae) originated in the late Miocene and evolved into one of the world's most successful carnivore families, inhabiting all the continents, except Antarctica [1]. Fossil and molecular data indicate that modern-day cat species evolved rapidly from a relatively recent common ancestor 10–15 million years ago (MYA). The family Felidae represents a unique evolutionary radiation, with numerous extant species exhibiting diverse ecological, morphological, and behavioral traits [2–5]. Their evolutionary history and divergence times have been disputed for many years because of rapid and very recent speciation events, few distinguishing dental and skeletal characteristics, incidents of parallel evolution, and an incomplete fossil record [1].

Morphological and molecular approaches have been used to disclose the evolutionary history of felines. Early efforts included overall morphological structure, comparative morphology, and comparative karyology [6–8], albumin immu-

*Corresponding author (email: wuxb@mail.ahnu.edu.cn)

nological distance, DNA-DNA hybridization, allozymes and two-dimensional protein electrophoresis [9–11], differential segregation of integrated retroviral sequences, sex chromosomes-linked genes, and chemical signals [12–14]. More recently, efforts to resolve phylogenetic relationships have focused on the mitochondrial genome [15], because the mitochondrial genome shows great variability in structure, gene content, organization, and mode of expression in the different organisms [16]. This extraordinary diversity probably reflects the different evolutionary pathways that gave rise to segregation of genetic information into different cellular compartments in the eukaryotic cell [16]. Mitochondrial DNA has become an important molecular marker and provides strong evidence in the study of phylogenetic relationships [17].

As the most recently evolved genus, there has been great confusion over the taxonomy and phylogeny of *Panthera* [11,18]. So far, the complete mtDNA sequences of only three feline species (*Felis catus, Acinonyx jubatus,* and *Neofelis nebulosa*) have been reported [17,19,20]. However, the data were not enough to explain the phylogenetic relationships of Felidae. The complete nucleotide sequences of the mitochondrial genomes of *Panthera uncia*, *Panthera pardus*, and *Panthera tigris* are reported in the present study for the first time. In comparison with the complete mitochondrial sequences of *N. nebulosa*, *F. catus*, and *A. jubatus*, we explored the mtDNA structural characteristics and *Panthera* evolution. In this paper, we will also clarify the phylogenetic position of *Panthera* based on combined datasets and the complete mtDNA sequence.

1 Materials and methods

1.1 Samples sources, DNA extraction and PCR amplification

Muscle samples of *P. pardus*, *P. tigris*, and skin of *P. uncia* were collected from Ningguo, Anhui province in China. The samples were stored at −80°C in the Animal Conservation Biology Laboratory, College of Life Sciences, Anhui Normal University.

Mitochondrial DNA of the three species was extracted from a piece of muscle and skin tissue using a GENMED mtDNA Extraction Kit. Two major steps, isolation of mitochondria and mitochondrial DNA extraction, were included (GENMED Scientifics Inc., USA). According to manufacturer's instructions, the step of crushing of the muscle and skin tissue was carried out under ice bath conditions. The other extraction steps were performed at 4°C. Agarose gel electrophoresis of the mtDNA sample with the total DNA showed no contamination from the chromosomal DNA. Based on the complete mtDNA sequences of *F. catus* (NC001700), *A. jubatus* (AY463959), and *N. nebulosa* (DQ257669), and some partial sequences of *P. tigris* (DQ151550), we successfully designed 34 pairs of primers for amplifying the complete mitochondrial genome sequences of the three species using Oligo 6.0 [21] (Table 1). PCR reactions were performed in an MJ Model PTC-200 thermal cycler with the following conditions: 95°C for 5 min; 30 cycles of 94°C for 50 s, 52°C–56°C for 1 min, 72°C for 1 min; and 72°C for 10 min. Each reaction included 19 μL sterile distilled water, 3 μL 10× PCR Buffer, 2 μL dNTP (2.5 mmol L^{-1}), 2 μL $MgCl_2$ (25 mmol L^{-1}), 1 μL of each primer (10 μmol L^{-1}), 1 unit of Taq DNA polymerase (Promega) and 1 μL of template for a total reaction volume of 30 μL. The resultant PCR fragments were subjected to electrophoresis on a 1% agarose gel.

1.2 Analyses of sequences data

The DNAs were purified from excised pieces of gel using DNA Gel Extraction Kit (Axygen) for sequencing on an automatic DNA sequencer (Applied Biosystems) from both strands using the primer walking method. Nucleotide sequences were edited using the program DNASTAR [22] and aligned by ClustalX [23]. The locations of the 13 protein-coding genes were identified using software SEQUIN and the two ribosomal RNA genes were determined by comparing the corresponding sequence of *F. catus* and homologous sequences of other Felidae mtDNAs. The tRNA genes were identified using software tRNA Scan-SE 1.21 (http://lowelab.ucsc.edu/tRNAscan-SE), and their cloverleaf secondary structure and anticodon sequences were predicted using DNASIS (Version 2.5, Hitachi Software Engineering). The complete nucleotide sequence of the mtDNA of *P. pardus*, *P. tigris*, and *P. uncia* were submitted to GenBank with the accession number EF551002, EF551003, and EF551004.

1.3 Molecular phylogenetic analyses

To further confirm the phylogenetic relationships among the *Panthera* genus, the complete mitochondrial DNAs of *N. nebulosa*, *A. jubatus*, *F. catus* and 7 mitochondrial genes of *Panthera onca*, *Panthera leo, Puma concolor*, and *Lynx lynx* were obtained from GenBank (Table 2). We constructed the phylogenetic tree based on 5 mitochondrial protein-coding genes (ND2+ND4+ND5+ATP8+Cyt *b*) (Combined sequences I), 7 mitochondrial segments (12S rRNA+16S rRNA+ND2+ND4+ND5+ATP8+Cyt *b*) (Combined sequences II) of 10 species, *Canis familiaris* was used as an outgroup. For the combined sequences, the base composition homogeneity was tested with chi-square (χ^2) tests for equal base frequencies across taxa; nucleotide saturation was analyzed by plotting the absolute number of transitions (Ti) and transversions (Tv) against absolute distance values. Transitions were deleted at the third positions of codons avoiding saturation problems caused by transitions.

Table 1 Primers for amplifying complete mtDNA genome of *P. pardus*, *P. tigris* and *P. uncia*[a)]

Primer name	Forward primer sequence (5′→3′)	Reverse primer sequence (5′→3′)	Annealing temperature
F1-U/D	TGAAAATGCCTAGATGAG	ATCTTCTGGGTGTAAGCC	54.0°C
F2-U/D	AATATGTACAYACCGCCCGTC	ATTACGCTACCTTYGCACG	54.5°C
F3-U/D	AACTCGGCAAACACAAGCC	TCGTTCAACTAGGGTTAGG	55.0°C
F4-U/D	TCAGAGGTTCAATTCCTC	TAGGATTAGGTTCGATTCC	54.0°C
F5-U/D	CAAGYATCCCACCTCAAAC	CAGCCTATATGGGCGATTG	55.0°C
F6-U/D	CCTACTCCTAACAATATCC	AGCAGTCCCTACTATACC	56.0°C
F7-U/D	CAGTCTAATGCTTACTCAGC	AGTATGCTCGTGTGTCTAC	55.0°C
F8-U/D	ATCGTCACCTACTACTCC	GTGGTCGTGRAAGTGTAG	55.0°C
F9-U/D	TGGTTTCAAGCCAATGCC	GATGTATCTAGTTGTGGC	54.0°C
F10-U/D	GTTCTTGAATTAGTYCCCC	GTTATAAGGAGGGCTGAAAG	53.0°C
F11-U/D	TGCTGTAGCCCTAATCCAA	TGTCTGTTTGTGAGGCTC	56.0°C
F12-U/D	TATGAGTGCGGATTTGACCC	CGTTCCGTTTGATTACCTC	53.0°C
F13-U/D	TCTAGTAGGCTCACTACC	GGTTCCTAAGACCAATGGA	52.0°C
F14-U/D	GAACTGCTAATTCATGCCTC	GTAGAAAYGCGAGGTAAG	53.0°C
F15-U/D	GCTATCTGTGCTCTCACAC	ARTAAGAGTARGCTGAGGG	54.0°C
F16-U/D	TGAGCCAAAARTCCGCATC	GTGCCAAAGTTTCATCAYG	53.5°C
F17-U/D	CCCTCAGAATGATATTTGTCCTCA	TGAGATCTGAAAAACCATCGTTG	53.0°C
F18-U/D	GCTCCTACACCTTCTCAG	GCACAGTATGGGTATATG	56.0°C
F19-U/D	TCAAGGAAGAAGCAACAGCC	GGTCATAGCTGAGTCATAGC	52.0°C
F20-U/D	ACTGTGGTGTCATGCATTTGG	GACTCATCTAGGCATTTTCAG	55.0°C
F21- U/D	GTCTCTCATTCTATTTATCGGGTC	GGGAATAATGCCTGTTGGT	53.0°C
F22- U/D	CGAGACATTATCCGAGAAA	TTCAGTTCACTCTAGTCCTT	52.0°C
F23- U/D	CACGAGAAAACGCCTAAT	GACCCAGAGCACATCAATAA	53.0°C
F24- U/D	ACCACCAGCCACAATCAAA	TGGATCGGAGGATTGCGTAT	52.0°C
F25- U/D	TCCAGGTCGGTTTCTATCTA	TAGGATGGGTGCTGTGATGAAT	53.1°C
F26- U/D	CTCTAAGTAAGCCCTATA	GCATGGGCAGTAACTACTA	55.0°C
F27-U/D	ACACCTATTCTGATTCTTCG	GAGAATTAAGATGATGGCTGGT	54.0°C
F28-U/D	TCAAGCCAATACCATAACCACT	TCCTATTATTGTTGGGGTA	53.0°C
F29-U/D	ACATGCCACAGTTAGATAC	TTTGAGTGATAGAAGGCCCAGA	53.0°C
F30-U/D	CCACTGCCATACTCATACCAAT	GTCTTTTGGTAGTCACAGGT	54.0°C
F31-U/D	ATAACACTTCATCTGCTCCCACT	TGTTAATGCGAGGCTTCCGATA	52.0°C
F32-U/D	TCCAGGCCCACCATAAATAG	CGTCCTACGTGCATGTATAGA	52.0°C
F33-U/D	CACGAGAAAACACCCTAA	GCGAGACTTCCGATGATGAG	52.0°C
F34-U/D	TCGCATTCTGATTACCCCAA	CTCTTTTGATTAGGTGTGACTG	55.0°C

a) Y=C or T, R=A or G, K=G or T, M=A or C, Respectively.

Table 2 Species in phylogenetic analyses

Scientific name	12S rRNA	16S rRNA	ND2	ND4	ND5	Cyt *b*	ATP8
Panthera uncia	EF551004	EF551004	EF551004	EF551004	EF551004	EF551004	EF551004
Panthera pardus	EF551002	EF551002	EF551002	EF551002	EF551002	EF551002	EF551002
Panthera tigris	EF551003	EF551003	EF551003	EF551003	EF551003	EF551003	EF551003
Panthera onca	AY012151	AF006441	AY634391	AY634403	AF006442	EF437582	DQ899924
Panthera leo	S9300	AF006457	AY170043	AY634398	AF006458	S79302	DQ899945
Neofelis nebulosa	DQ257669	DQ257669	DQ257669	DQ257669	DQ257669	DQ257669	DQ257669
Acinonyx jubatus	AY463959	AY463959	AY463959	AY463959	AY463959	AY463959	AY463959
Puma concolor	U33495	AF006455	AY634392	AY634404	AF006456	AY598487	AY598483
Lynx lynx	D28891	AF006413	AY634389	AY634401	AF006414	AY773083	AY598471
Felis catus	NC_001700	NC_001700	NC_001700	NC_001700	NC_001700	NC_001700	NC_001700
Canis familiaris	U96639	U96639	U96639	U96639	U96639	U96639	U96639

The data sets were subjected to 3 different methods of phylogenetic reconstruction: MP (maximum parsimony), maximum likelihood (ML), and the Bayesian, respectively. Both maximum parsimony (MP) and maximum likelihood (ML) were used to construct phylogeny relationships. MP and ML analyses were complete with PAUP*4b10 [24] with the heuristic search option using 100 random addition sequence replicates and tree bisection-reconnection (TBR)

branch swapping. All characteristics were treated as un-ordered. Bootstrap branch support (BBP) values were estimated using 1000 nonparametric bootstraps (BS) with heuristic searches involving 50 random addition sequence replicates. Bootstrap values had to be >70% to be sufficiently supported, and those with values between 50% and 70% were considered as weakly supported [25].

Bayesian analyses were performed using MrBayes 3.0b4 [26]. Prior to the analyses, the best-fit model of DNA substitution was estimated using ModelTest ver.3.6 [27] and a general-time-reversible+gamma+invariant (GTR+I+G, G= 1.8671, I=0.5549) model proposed under the nested likelihood ratio model and AIC (Akaike Information Criterion) consideration. Three independent iterations were run for 4×10^6 generations, and sampled every 100 generations, and the first 4×10^6 generations (10%) discarded as burn-in. Parameters were plotted against generations to check that convergence had been reached well before the post burn-in portion of the data. The remaining trees were used to construct a 50% majority rule consensus tree. For the Bayesian analyses, we used posterior probabilities as indicators of node confidence. As these represent the true probabilities of the clades [28], probabilities >95% were considered to be significant [29].

1.4 Testing phylogenetic hypotheses

The convergence of the phylogenetic trees produced by different analysis methods was compared using the Shimodaira-Hasegawa test (SH test) [30]. The SH test was used to test optimal phylogenetic tree selection. The tests were performed in PAUP*4.0b10 with the GTR+I+G model selected by the nested likelihood ratio model and AIC.

1.5 Divergence time estimation

NADH dehydrogenase subunit 6 gene (ND6) is the only protein-coding gene encoded on the light strand and thus differs in nt and aa composition from other protein-coding gene, it shows distinct mutational biases and influences replacement patterns at the amino acid sequence level [31,32]. The control region of animal mtDNAs usually accumulates base substitutions and indels at high rates [33]. Therefore ND6 and the control region were not used in the estimation of divergence dates. In addition, one of the important factors that determine the accuracy of estimates of divergence times is reliability of the calibration point used for producing the time scale of the phylogenetic tree constructed [34]. In this study, we used four well-established vertebrate calibration points for the divergence time estimation: felid and canids (55 MYA) [35], *Equus caballus* and *Rhinoceros unicornis* ((55±1.5) MYA) [36], *Aythya americana* and *Gallus gallus* (68 MYA) [36], *Didelphis virginiana* and *Macropus robustus* (70–60 MYA) [37]. These dates are consistent with the fossil record.

To test the assumption of a global clock-like evolution in the DNA sequences surveyed, the likelihood-ratio test (LRT) [38] was calculated separately, with and without molecular clock constraints for ML analysis, respectively. If the results were notably different, the molecular clock would be rejected. LRT ($\chi^2 = 1534.024$, d$f = 31$, $P < 0.001$) showed that the difference was great. Therefore the molecular clock assumption of complete mitochondrial DNA genes data set except the ND6 gene and D-loop region was rejected, and the global clock was not suitable to calculate the divergence time in this study.

Thus, Maximum Likelihood (ML) branch lengths used by Janke and Arnason [39], based on the complete mitochondrial genome (except the NADH6 gene and the control region), which allows different parts of a tree to have different rates, were performed to infer the divergence time of the genus *Panthera*. Moreover, the divergence times were also calculated and tested based on four well-established vertebrate calibration points by the program MEGA 3.1 [40]. The complete mitochondrial genomes of 21 vertebrates were used in this study (Table 3).

2 Results

2.1 Characteristics of the two combined sequences

The mean base composition in combined sequences I and combined sequences II were AT-biased at 60.1% and 59.5%, respectively and had a low G content at 11.7% and 13.8%, respectively. Significant compositional biases exist at the

Table 3 Complete mtDNA sequences used in this study

Name of species	Accession number of GenBank	References
Panthera uncia	EF551004	This study
Panthera pardus	EF551002	This study
Panthera tigris	EF551003	This study
Felis catus	NC001700	[19]
Acinonyx jubatus	AY463959	[20]
Acinonyx jubatus	AF344830)	[20]
Neofelis nebulosa	DQ257669	[17]
Canis familiaris	U96639	[44]
Ursus maritimus	AJ428577	[71]
Equus asinus	X97337	[43]
Equus caballus	X79547	[72]
Ceratotherium simum	Y07726	[73]
Rhinoceros unicornis	X97336	[74]
Didelphis virginiana	Z29573	[75]
Macropus robustusm	Y10524	[39]
Gallus gallus	X52392	[76]
Aythya americana	AF090337	[77]
Rhea americana	AF090339	[78]
Struthio camelus	Y12025	[79]
Alligator mississippiensis	Y13113	[80]
Alligator sinensis	AF511507	[81]

second and, especially, the third codon positions, where there was a marked under representation of guanine, while base composition at the first codon positions was almost equal. After alignment, there were 3300 and 4538 bases for the two combinations. In total, 1205 and 1360 variable sites were detected for the two combinations, of which, 793 and 857 were parsimony-informative sites, and the transition/transversion ratios (ti/tv) were 5.66 and 5.08, respectively. The two combined sequences generated strong phylogenetic information. The characteristics of the two combined sequences are summarized in Table 4.

2.2 Complete mitochondrial genomes content and structure

The complete mitochondrial genome sequences of *P. pardus*, *P. tigris*, and *P. uncia* were reported for the first time. The complete mitochondrial genomes of *P. pardus*, *P. tigris*, and *P. uncia* were determined to be 16964, 16990, and 16773 bp long, respectively. Each of the three mitochondrial DNA genomes included 13 protein-coding genes, 22 tRNA, two rRNA, one O_LR, and one control region. There are 28 genes encoded by the majority-strand (H-strand), and nine genes by the minority-strand (L-strand). The structures of these mitochondrial genomes are highly similar to those of *F. catus*, *A. jubatus*, and *N. nebulosa* (Figure 1 and Table 5). The mitochondrial genome composition in *P. pardus, P. tigris*, and *P. uncia* were AT-rich biased. The base composition of the H-strand was A: 31. 9%; T: 26.9%; C: 26. 6%; G: 14.6% for *P. tigris*; A: 31. 8%; T: 27.4%; C: 26. 6%; G: 14.5% for *P. pardus*; and A: 31. 9%; T: 27.1%; C: 26. 5%; G: 14.5% for *P. uncia.*

2.3 Protein-coding genes

All 13 protein-coding open reading frames (ORFs) are included in the mtDNA of *P. pardus, P. tigris*, and *P. uncia* mitochondrial genomes, with the same organization and no major rearrangement, which are found in other mammalian mitochondrial genomes. The longest ORF was the ND5 gene (1821 bp for *P. pardus*, 1830 bp for *P. tigris* and *P. uncia*), while the shortest ORF was the ATP8 gene (204 bp). All of the protein-coding genes were encoded by the H-strand, except for ND6, which is encoded by the L-strand. There were no introns in these genes. There are nine protein-coding genes in *P. pardus, P. tigris*, and *P. uncia* mitochondrial genome (COI, COII, ND4, ND4L, ND5, ND6 ATPase 6, ATPase 8, and CYT *b*) with ATG as the initiation codon. The ND3 and ND5 genes are initiated by an ATA codon, the ND2 gene is initiated by ATC, and only the COIII gene is initiated by an ATA codon for *P. uncia*. The termination codons are all TAA, except Cyt *b* with AGA, ND3 with TA, and COIII, ND2, and ND4 with a single T (The termination codon of COIII was TAA for *P. uncia*). The ND2, COIII, ND3, and ND4 genes of *P. pardus* and *P. tigris* lack complete termination codons. As in the transcripts of the human peptide-coding mitochondrial genes, ND1, ND2, CO3, and ND3 contain a stop codon created by posttranscriptional polyadenylation. Therefore, most stop codons in the three mtDNAs appear to be TAA (Table 5). As in other vertebrate mtDNAs, coding sequences overlapped between ATP8 and ND6, between ND4 and ND4L, and between ND5 and ND6.

The base usage of *P. pardus, P. tigris*, and *P. uncia* protein-coding genes are shown in Tables 6 and 7. Base A was the most frequent nucleotide in protein-coding genes (average contents were 30.9% for *P. tigris*, 31.5% for *P. pardus*,

Table 4 Summary statistics for mitochondrial genes used in this study[a)]

	mtDNA datasets	
	Combined sequences I	Combined sequences II
Aligned sites (bp)	3300	4538
A%	33. 0	33. 6
C%	28.2	26. 8
G%	11.7	13. 8
T%	27.1	25. 9
Conserved sites	2095 (63.48%)	3178 (81.93%)
Variable sites	1205 (36.52%)	1360 (29.97%)
Parsimony informative sites	793 (24.03%)	857 (18.88%)
Ti : Tv ratio	5.66	5.08
Pairwise distance (%) within group	12.04 (6.8–16.5)	9. 06 (5.8–13.0)

a) Combined sequences I: ND2 + ND4 + ND5 + ATP8 + Cyt *b*. Combined sequences II: 12S rRNA +16S rRNA + ND2 + ND4 + ND5 + ATP8 + Cyt *b*.

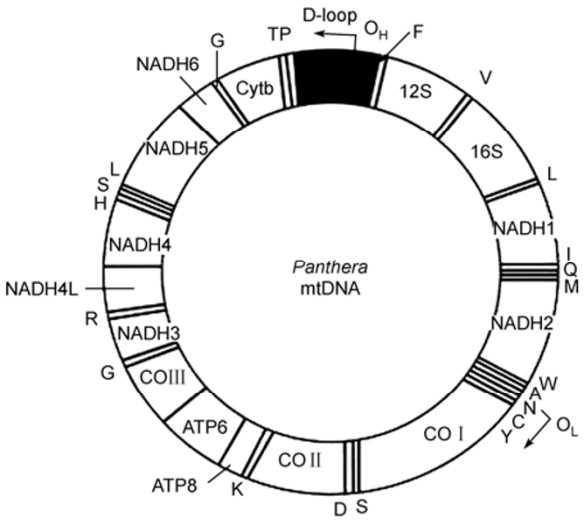

Figure 1 Complete mitochondrial (mt)DNA organization of *P. tigris*, *P. pardus*, and *P. uncia*. Gene abbreviations used are 12S, 12S rRNA; 16S, 16S rRNA; NADH1-6, NADH dehydrogenase subunits 1–6; COI–III, cytochrome oxidase subunits I–III; ATP6 and ATP8, ATPase subunits 6 and 8; cyt *b*, cytochrome b; Transfer (t)RNA genes are identified by a single letter of the amino acid codon. O_H and O_L stand for the heavy-strand replication origin and the light-strand replication origin, respectively.

Table 5 Organization of the mitochondrial genomes of *P. tigris, P. pardus* and *P. uncia*[a)]

Gene	Position			Start codon	Stop codon	H/L Strand
	P. tigris	*P. pardus*	*P. uncia*			
D-loop	1-927	1-954	1-743			H
$tRNA^{Phe}$	928-998	955-1025	744-813			H
12S rRNA	999-1958	1026-1984	814-1773			H
$tRNA^{Val}$	1959-2026	1985-2052	1774-1841			H
16S rRNA	2027-3601	2053-3624	1842-3421			H
$tRNA^{Leu(UUR)}$	3602-3676	3625-3701	3422-3496			H
ND1	3679-4635	3704-4660	3499-4455	ATG	AGA/TAA	H
$tRNA^{Ile}$	4635-4703	4660-4728	4455-4523			H
$tRNA^{Gln}$	4701-4774	4726-4799	4521-4594			L
$tRNA^{Met}$	4775-4843	4801-4869	4596-4664			H
ND2	4844-5885	4870-5911	4665-5706	ATC/ATT	T/TAG	H
$tRNA^{Trp}$	5886-5954	5912-5980	5707-5775			H
$tRNA^{Ala}$	5970-6038	5997-6065	5792-5860			L
$tRNA^{Asn}$	6040-6112	6067-6139	5862-5934			L
O_LR	6113-6145	6140-6178	5935-5966			L
$tRNA^{Cys}$	6146-6210	6179-6244	5967-6032			L
$tRNA^{Tyr}$	6211-6278	6238-6303	6033-6097			L
COI	6280-7824	6305-7849	6099-7643	ATG	TAA	H
$tRNA^{Ser(UCN)}$	7822-7890	7847-7915	7641-7709			L
$tRNA^{Asp}$	7897-7965	7922-7990	7716-7784			H
COII	7966-8649	7922-8674	7785-8468	ATG	TAA	H
$tRNA^{Lys}$	8653-8720	8678-8745	8472-8539			H
ATP8	8722-8925	8747-8950	8541-8744	ATG	TAA	H
ATP6	8883-9563	8908-9588	8702-9382	ATG	TAA	H
COIII	9563-10346	9588-10371	9361-10140	ATG	T/TAA	H
$tRNA^{Gly}$	10347-10415	10372-10440	10166-10234			H
ND3	10416-10762	10441-10787	10235-10581	ATA	TA	H
$tRNA^{Arg}$	10763-10831	10788-10856	10582-10650			H
ND4L	10832-11128	10857-11153	10651-10947	ATG	TAA	H
ND4	11122-12499	11147-12523	10941-12318	ATG	T	H
$tRNA^{His}$	12500-12568	12525-12593	12319-12387			H
$tRNA^{Ser(AGY)}$	12570-12628	12600-12657	12388-12446			H
$tRNA^{Leu(CUN)}$	12629-12698	12653-12722	12447-12516			H
ND5	12690-14519	12723-14543	12508-14337	ATA	TAA	H
ND6	14503-15030	14527-15054	14321-14848	ATG	TAA	L
$tRNA^{Glu}$	15031-15099	15055-15123	14849-14917			L
Cyt *b*	15103-16242	15127-16266	14921-16060	ATG	AGA	H
$tRNA^{Thr}$	16243-16312	16271-16340	16061-16130			L
$tRNA^{Pro}$	16313-16379	16337-16403	16131-16197			H
D-loop	16380-16990	16404-16964	16198-16773			H

a) L, light strand.

and 28.7% for *P. uncia*), with T and C following. Similar to other vertebrates, the base composition of *P. pardus, P. tigris*, and *P. uncia* protein-coding genes was biased against G (the average content was 13.3% for *P. tigris*, 11.4% for *P. pardus*, and 14.0% for *P. uncia*). The A + T contents were higher than the C + G contents in the first, second, and third position codons of protein-coding genes, which is consistent with the A+T content-rich of the mt genome.

2.4 Control region

The control region (CR) of the three mitochondrial DNA genomes is located between $tRNA^{Pro}$ and $tRNA^{Phe}$, and contains only promoters and regulatory sequences for replication and transcription, but no structural genes. Tandem repeats generally occur in this region. Jae-Heup *et al.*[41] studied the control region of *Panthera* species and divided it into three parts: the left domain, the central conserved region (CCR), and the right domain. The hypervariable segment (HVS)-1 and the repetitive sequence (RS)-2 are in the left domain, whereas RS-3 and HVS-2 are in the right domain. Conserved sequence block (CSB)-2 and CSB-3 are in HVS-2. CSB-1 is in the CCR, which is located between RS-2 and RS-3. By comparing the CR sequences of the

Table 6 Base composition in protein-coding genes of *P. tigris*, *P. pardus*, and *P. uncia*

Gene	*P. tigris*,				*P. pardus*				*P. uncia*			
	T %	C %	A %	G%	T %	C %	A%	G%	T%	C %	A %	G%
ND1	27.0	30.2	30.9	11.8	26.3	31.0	30.1	12.5	25.9	31.8	29.9	12.4
ND 2	25.0	29.2	35.7	9.9	24.6	29.6	35.9	9.9	25.2	29.1	36.4	9.3
ND 3	25.9	31.2	30.5	12.4	28.8	28.2	30.3	12.7	27.2	29.8	31.2	11.8
ND4L	30.9	25.9	28.6	14.5	31.4	25.2	30.9	12.5	31.1	24.5	29.3	14.1
ND 4	27.5	28.9	31.5	12.1	27.2	29.2	31.3	12.3	27.5	28.7	31.3	12.5
ND 5	27.8	28.7	31.0	12.5	28.5	28.4	31.2	11.9	28.0	28.5	31.4	12.1
ND 6	20.6	29.5	38.1	11.7	21.8	28.4	39.0	10.8	20.3	29.7	40.0	10.0
COI	31.0	23.9	26.0	19.1	31.7	23.2	26.7	18.4	32.1	22.9	26.0	19.0
CO II	27.5	25.9	30.6	16.0	26.9	26.8	31.1	15.2	27.2	26.3	31.9	14.6
CO III	28.2	28.4	26.8	16.6	28.9	28.2	26.7	16.2	28.1	28.0	28.5	15.4
ATP8	26.5	25.5	38.7	9.3	27.5	25.0	41.2	5.9	27.5	25.5	38.7	8.3
ATP 6	30.4	28.0	29.0	12.6	30.2	28.0	28.0	13.8	29.2	28.8	29.5	12.5
Cytb	27.4	30.3	27.9	14.5	27.8	30.0	27.4	14.8	26.7	23.5	27.8	14.5
Avg	27.4	28.1	30.9	13.3	27.8	26.0	31.5	11.4	27.4	27.5	28.7	14.0

Table 7 Base usage in protein-coding genes of *P. tigris*, *P. pardus* and *P. uncia*

Gene	*P. tigris*			*P. pardus*			*P. uncia*		
	1st codon (A+T)%	2nd codon (A+T)%	3rd codon (A+T)%	1st codon (A+T)%	2nd codon (A+T)%	3rd codon (A+T)%	1st codon (A+T)%	2nd codon (A+T)%	3rd codon (A+T)%
ND1	50.78	57.99	61.75	50.67	57.96	61.77	50.74	57.94	61.77
ND 2	63.68	61.67	59.36	63.35	61.68	59.38	63.67	61.68	59.38
ND 3	47.82	60.00	60.00	47.65	60.01	60.08	47.84	60.06	60.02
NDL	54.54	69.69	54.54	54.54	69.68	54.52	54.56	69.69	54.52
ND 4	53.14	60.00	61.44	53.21	60.02	61.44	53.17	60.10	61.42
ND 5	57.86	62.45	54.91	57.84	62.46	54.90	57.88	62.47	54.94
ND 6	61.36	57.38	53.41	61.42	57.36	53.40	61.32	57.39	53.42
COI	49.71	58.44	61.75	49.82	58.45	61.73	49.73	58.42	61.77
CO II	50.43	64.04	58.33	50.54	60.06	58.34	50.44	64.08	58.35
COIII	51.72	57.09	54.79	51.68	57.10	54.72	51.76	57.07	54.78
ATP8	63.24	60.29	72.06	63.21	60.30	72.06	63.23	60.28	72.08
ATP6	50.66	62.11	64.32	50.61	62.13	64.36	50.68	62.16	64.34
Cytb	52.37	60.53	52.37	52.32	60.52	52.37	52.38	60.56	52.38
Avg	54.41	60.89	59.17	54.52	60.59	59.16	54.42	60.92	59.16

three mitochondrial DNA genomes with those of *F. catus*, *A. jubatus*, and *N. nebulosa*, we identified a central conserved region, a left domain with HVS-1 and RS-2 at the 5′ end, and a right domain with HVS-2 and RS-3 at the 3′ end of the control region. The CCR between the end of RS-2 and the beginning of RS-3 ranged from 476 to 477 bp among the three species. *P. tigris* had the longest HVS-1 segment (248 bp), followed by *P. uncia* (214 bp), and *P. pardus* (200 bp). There are some repetitive sequences in the CR, such as 5′-ACACACGTACACACGT-3′, which repeats 14, 11 and 2 times in the control region of *P. pardus*, *P. tigri*s and *P. uncia*, respectively.

2.5 Ribosomal and transfer RNA genes

Located between $tRNA^{Phe}$ and $tRNA^{Val}$, the 12S rRNA genes of *P. tigri*s, *P. pardus*, and *P. uncia* are 960, 959 and 960 bp, similar to *F. catus*, *A. jubatus*, and *N. nebulosa*. However, they are more conserved than those of *F. catus* and *A. jubatus*, and only 79, 85, and 71 sites are variable, accounting for 8.2%, 8.8%, and 7.6% respectively. The 16S rRNA genes, located between $tRNA^{Val}$ and $tRNA^{Leu\ (UUR)}$, are 1575, 1572, and 1580 bp, respectively. They are more conserved than the 12S rRNA genes, with only 113, 114, and 115 variable sites, accounting for 7.1%, 7.2%, and 7.1%, respectively. A total of 22 tRNAs were found in the mtDNA of the three species, including $tRNA^{Leu\ (UUR)}$, $tRNA^{Leu(CUN)}$, $tRNA^{Ser\ (UCN)}$, and $tRNA^{Ser\ (AGY)}$.

2.6 Phylogenetic reconstruction

2.6.1 Phylogenetic analyses based on five protein-coding genes combined

ML, MP, and Bayesian trees derived from analyses of ND2, ND4, ND5, ATP8, and Cyt *b* combined datasets are shown in Figure 2. The monophyly of the genus *Panthera*, includ-

ing *P. leo, P. uncia*, *P. pardus*, *P. onca. P. tigris,* and *N. nebulosa*, was strongly supported by the combined five protein-coding genes. ML, MP, and Bayesian trees provided high bootstrap values for *N. nebulosa* as the basal member of the genus *Panthera*. However, the internal relationships showed more change. It was notable that the identification of *P. leo* and *P. uncia* as sister species was strongly supported by ML, MP, and Bayesian analyses. The precise placement of *P. tigris* as a sister-group of the other four species (*P. leo*, *P. onca*, *P. pardus*, and *P. uncia*) was clearly upheld in the ML and MP tree. However, the relationships among *P. onca*, *P. pardus*, and the sister species (*P. leo*, *P. uncia*) were not robust; the support values for *P. pardus* paired with the other two species (*P. leo*, *P. uncia*) were only 42%, 65% 0.78 in MP, ML and Bayesian trees. The support for *P. onca* as the sister-group to three *Panthera* species (*P. pardus*, *P. leo*, and *P. uncia)* were 87% and 72% in the MP and ML tree.

2.6.2 Phylogenetic analyses based on seven combined mitochondrial genes

Combined data of seven mtDNA genes (12S rRNA, 16S rRNA, ND2, ND4, ND5, Cyt b, and ATP8) were also used to reconstruct the phylogenetic trees by MP, ML, and Bayesian methods. The MP, ML, and Bayesian bootstrap majority consensus trees from this dataset are presented in Figure 3. ML, MP, and Bayesian trees all suggested that *N. nebulosa* should be included within *Panthera* genus. ML, MP, and Bayesian tree provided strong support for *P. uncia* paired with *P. leo*. However, the combined dataset exhibited moderate resolution and nodal support for *P. onca*, and weak nodal support for *P. pardus*.

2.6.3 Phylogenetic analyses based on the complete mitochondrial genomes

The ML and Bayesian analyses based on 21 complete mitochondrial genomes, including six cat species, yielded the same topology (Figure 4). The six cat species split into two groups, one containing *N. nebulosa*, *P. tigris*, *P. pardus*, and *P. uncia*, and another containing *F. catus* and *A. jubatus*. In the former clade, *N. nebulosa* occupied the most basal position, followed by *P. tigris* and lastly the two sister species *P. pardus*, and *P. uncia* (ML, 100%; Bayesian, 1.00).

2.7 Estimates of divergence dates

Divergence times were estimated based on Maximum Likelihood (ML) branch lengths; the lengths of various branches

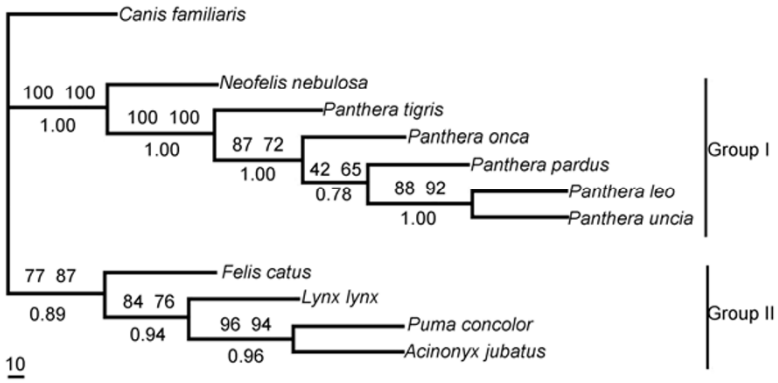

Figure 2 Phylogenetic relationships based on analyses of combined ND2+ATP8+ND4+ND5+Cyt *b*. ML, MP, and Bayesian analyses obtained similar tree topologies. Bootstrap values are above the branches; Bayesian probabilities are below the branches.

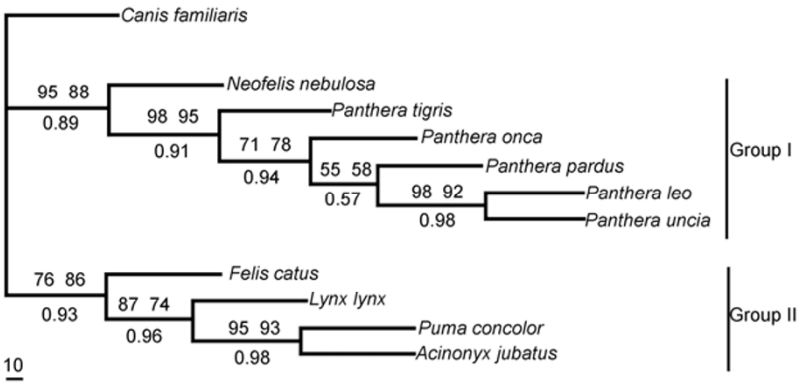

Figure 3 Phylogenetic relationships based on analyses of combined 12S rRNA+16S rRNA+ND2+ATP8+ND4+ND5+Cyt *b*. ML, MP, and Bayesian analyses obtained similar tree topologies. Bootstrap values are above the branches; Bayesian probabilities are below the branches.

of the tree are shown in Table 8. The estimates were performed by applying two calibrations: felid and canids (55 MYA), and *E. caballus* and *R. rhinoceros* (55 ± 1.5 MYA). The divergence time between the genus *Panthera* and other felid species can be expressed as: the genus *Panthera* branch×55/the genus *Panthera* branch + branch M, where 55 represents the time, 55 MYA. This calculation yields a divergence time of ~11.3MYA. Then, based on inferring dating information from molecular phylogenies and ages of fossil constraint, we estimated the divergence times for *N. nebulosa* (8.66 MYA), *P. tigris* (6.55 MYA), *P. uncia* (4.63 MYA), and *P. pardus* (4.35 MYA) by the same method. Moreover, we tested our results using the program MEGA 3.1 using four well-established vertebrate calibration points. In particular, the divergence event and radiation of *P. uncia*, which is a unique species of the Qinghai-Tibetan Plateau,

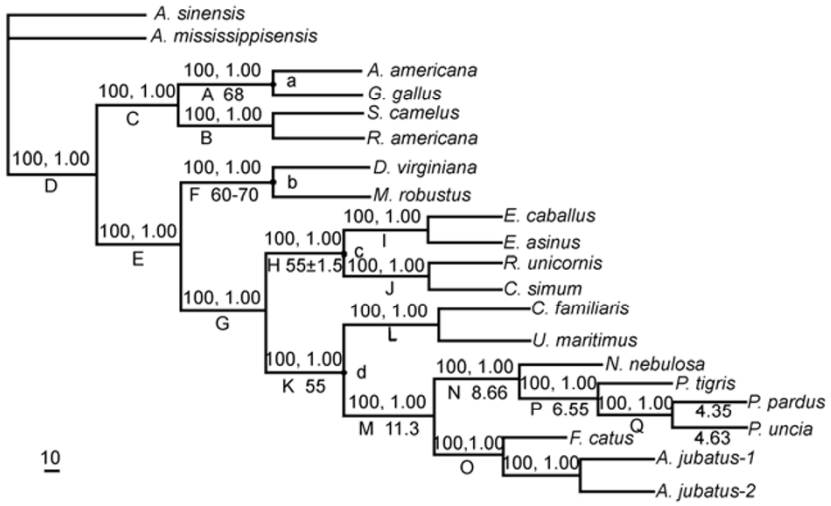

Figure 4 ML and Bayesian tree based on 21 complete mtDNA sequences (except the NADH6 gene and the control region). Divergence time of the genus *Panthera* was estimated based on Maximum likelihood branch lengths (A-Q) (Table 8) and four calibration points: (a) 68 MYA for Anatidae/Phasianidae [36]; (b) 70-60 MYA for *D. virginiana*/*M. robustus* [37]; (c) (55 ± 1.5) MYA for Equidae/Rhinocerotidae [35]; and (d) 55 MYA for Felid/Canids [35]. Numbers above the branches indicate bootstrap values of ML and Bayesian probabilities. Numbers directly below the branches represent divergence times.

Table 8 Maximum-Likelihood (ML) branch lengths[a)]

External	Length	SE	Internal	Length	SE
A. americana	0.11411	0.00339	A	0.03384	0.00293
G. gallus	0.11442	0.00341	B	0.03521	0.00239
S. camelus	0.10153	0.00318	C	0.11582	0.00428
R. americana	0.09381	0.00307	D	0.09237	0.00344
D. virginiana	0.14865	0.00413	E	0.22038	0.00565
M. robustus	0.11490	0.00374	F	0.09510	0.00378
E. caballus	0.03373	0.00178	G	0.12144	0.00441
E. asinus	0.03821	0.00187	H	0.03688	0.00229
R. unicornis	0.06028	0.00238	I	0.06418	0.00257
C. simum	0.05701	0.00231	J	0.04222	0.00218
C. familiaris	0.11648	0.00344	K	0.08233	0.00356
U. maritimus	0.12463	0.00353	L	0.03632	0.00228
A. jubatus	0.05731	0.00223	M	0.06636	0.00229
F. cats	0.04916	0.00208	N	0.01944	0.00156
P. pardus	0.03525	0.00174	O	0.01781	0.00149
P. uncia	0.04312	0.00189	P	0.01731	0.00146
P. tigris	0.04907	0.00206	Q	0.01611	0.00129
N. nebulosa	0.06168	0.00229			
A. mississippiensis	0.10641	0.00358			
A. sinensis	0.09238	0.00346			

a) Calculation of ML branch lengths and standard errors (SE) were based on the tree in Figure 2C. The tree was established by analysis of 21 complete mtDNA sequences (except the NADH6 gene and the control region).

mostly correlated with the geological tectonic events and intensive climate shift that happened at 8, 3.6, 2.5, and 1.7 million years ago (MYA) of the late Cenozoic period.

3 Discussion

3.1 General features of genus *Panthera* mtDNA

Similar to other mammals, base G was is used the least of the four bases, while A is used the most; the three mtDNA genomes are AT rich. In fact, AT bias is distinctly observed in the mtDNA of vertebrates, especially in the control region [42]. The same case was found in *F. catus*, *A. jubatus*, and *N. nebulosa*.

Protein translation is generally initiated by the start condon ATG (Met), similar to the initial codons of most vertebrate mitochondrial protein-coding genes [43], except for ND2, which uses ATC (Ile), and ND3/ND5, which use ATA. It was noticeable that the stop codons of the Cyt *b* gene in three felids are all AGA, which is different from other protein-coding genes. This case occurs in most mammals, such as canis [44] and rabbit [45]. However, the Cyt *b* genes are often terminated with T, TA, TAA or by no stop codon in amphibians [46], reptiles [47] and Aves [42]. Therefore, the Cyt *b* gene seems to tend to terminate with AGA in the mtDNA of mammals, which is distinctive from other families, while the start and stop codons in the other protein-coding genes are often unbiased among species.

The typical length of tRNA genes is about 59–75 bp in vertebrates [19,20]. In the three mtDNA genomes, the shortest tRNA is $tRNA^{Ser(AGY)}$ and the longest one is $tRNA^{Asn}$. All the tRNAs in the three genomes could be folded into a cloverleaf secondary structure, as in most other mammals, the only exception is $tRNA^{Ser(AGY)}$ that lacks the ''DHU'' arm [48].

3.2 Monophyly and phylogenetic placement of *Neofelis nebulosa*

Until now, several different hypotheses (Table 9) existed for the phylogenetic relationships in the genus *Panthera*. Traditionally, the genus *Panthera* consisted of *P. tigris*, *P. uncia*, *P. pardus*, *P. leo*, *P. onca* and excluded *N. nebulosa*. These species have been classified into the same genus because of a specialized jaw structure (flexible hyoid process) that consistently appears in most members of this group. The relationship between *N. nebulosa* and *Panthera* was also observed in prior studies. *N. nebulosa* has been placed within the genus *Panthera* as the sixth species based on morphological and molecular data [15,49]; King *et al.*[50] and O'Brien *et al.*[51] obtained the same result based on the SRY (sex-determining region on the Y chromosome) gene and Genomic paw prints. The possible sister species status of *N. nebulosa* and *P. tigris* was proposed by Janczewski *et al.*[18] from mt 12SrRNA and cyt *b*. However, *N. nebulosa* was included within *Panthera* genus as sister species of (*P. leo* (*P. pardus*, *P. uncia*)) by Yu *et al.*[52] based on the sequences of two nuclear DNA genes. Phylogenetic analyses in the present study were deduced from combined mtDNA sequences using MP, ML, and Bayesian method, and resulted in a new monophyly relationship of the *Panthera* genus: *N. nebulosa* (*P. tigris* (*P. onca* (*P. pardus* (*P. leo*, *P. uncia*)))) (Figures 2–4). *N. nebulosa* consistently occupied the most basal position in MP, ML, and Bayesian trees (Bootstrap values 100%, Bayesian probabilities 1.00). Our analyses support the view that *N. nebulosa* should be included within the *Panthera* genus as the basal member.

3.3 Interspecific relationship of the genus *Panthera*

The evolutionary relationships of the species within the ge-

Table 9 Evidence from previous studies phylogenetic relationship among the genus *Panthera*

Evidence	Phylogeny	Reference
Morphology	*P. uncia*, *P. tigris*, (*P. pardus*, *P. leo*, *P. onca*)	[56]
Morphology	*P. uncia* (*P. tigris* (*P. pardus*, *P. leo*, *P. onca*))	[8]
Molecular	(*N. nebulosa*, *P. tigris*) ((*P. uncia*, *P. onca*) (*P. pardus*, *P. leo*))	[18]
Molecular	*N. nebulosa* (*P. uncia* (*P. tigris*, *P. onca*, *P. pardus*, *P. leo*))	[15]
morphological, molecular	*N. nebulosa* (*P. uncia* (*P. tigris* (*P. onca* (*P. pardus*, *P. leo*))))	[49]
Molecular, Morphology and Karyological	*N. nebulosa* (*P. uncia* (*P. pardus* (*P. leo* (*P. tigris*, *P. onca*))))	[60]
Chemical signals	(*P. tigris*, *P. uncia*) (*P. onca* (*P. pardus*, *P. leo*))	[14]
Molecular	(*P. tigris*, *P. uncia*) (*P. onca* (*P. pardus*, *P. leo*))	[41]
Molecular	*N. nebulosa* (*P. tigris* (*P. onca* (*P. leo* (*P. uncia P. pardus*))))	[58]
Molecular	*N. nebulosa* ((*P. uncia P. tigris*) (*P. pardus* (*P. leo* , *P. onca*)))	[1]
Molecular	*N. nebulosa* (*P. leo* (*P. uncia* (*P. pardus* (*P. onca*, *P. tigris*))))	[61]
Molecular	*N. nebulosa* (*P. tigris* (*P. uncia* (*P. onca*, *P. leo*, *P. pardus*)))	[59]
Molecular	*P. tigris* (*N. nebulosa* (*P. leo* (*P. uncia P. pardus*)))	[52]
Molecular	*N. nebulosa* (*P. uncia*, *P. tigris*, *P. pardus, P. leo*, *P. onca*)	[50]
Molecular	*N. nebulosa* ((*P. tigris*, *P. uncia*) (*P. onca* (*P. pardus*, *P. leo*)))	[51]
Molecular	*N. nebulosa* ((*P. tigris*, *P. uncia*) (*P. onca*, *P. pardus*, *P. leo*))	[62]

nus *Panthera* have been the focus of intensive study for many years. However, some of the most important relationships at the species level within this group were still unresolved due to the extremely recent speciation (1–2 MYA) [53,54]. For instance, the earliest *Panthera* fossil from the East African Pleistocene (2 MYA) displayed a close relationship between *P. leo* and *P. tigris*. Neff [55] and Hemmer [56] thought that *P. leo* and *P. onca* were closer according to a fossil of the North American lion, *Panthera atrox* (30000 years old), as well as a fossil of a European Pleistocene cat, *Panthera gombaszoegensis* (2 MYA). Pocock [57], however, suggested that *P. pardus* and *P. onca* exhibit a close relationship based on morphological characteristics of extant representatives. Some controversy still exist on whether or not *P. uncia* should be included in the genus *Panthera*, because it lacks the flexibility in the hyoid process and because of morphological similarities to *A. jubatus*, which also lacks this specialization.

Based two combined sequences, MP, ML, and Bayesian methods of phylogenetic analyses consistently yielded a tree with the same topology (Figures 2 and 3) in this study. The 10 cat species used in the phylogenetic analyses were divided into two supported major groups. Group I comprised 6 species. *N. nebulosa* occupied the most basal position at the branch of the tree, followed by *P. tigris*, *P. onca*, *P. pardus*, and then last two most recently diverged sister species, *P. leo* and *P. uncia*. Group II contained three pantherine cats and the domestic cat. Our analyses indicated that *N. nebulosa* was included within the *Panthera* genus. *P. tigris* was the sister taxon to the other members of *Panthera* within the clade, which contains the other members of the genus; The position of *P. tigris* and *P. onca* were different from the previous molecular analysis obtained by Yu *et al.* [58] and Pecon-Slattery *et al.*[59] (Table 9). *P. pardus* was weakly supported as the sister taxon to *P. leo* and *P. uncia* in MP, ML, and Bayesian trees. The most interesting and novel finding of this study was that *P. uncia* and *P. leo* are probably sister species; this relationship was supported by MP and ML bootstrap values, and by Bayesian probabilities based on combined sequences. Many biologists have studied the evolution and phylogeny of *P. uncia* in previous studies. *P. uncia* was placed as the most basic taxon in genus *Panthera* by Johnson and O'Brien *et al.* [15] using partial mt16S rRNA and ND5 genes. Mattern and McLennan [60] obtained the same result based on partial mt12S and 16S rRNA, ND5, and Cyt *b* genes combined with morphological and karyological characters. Yu *et al.* [58] suggested that *P. uncia* and *P. pardus* was sister species based on the combined analysis of six genes (ND2, ND4, ND5, cytb, 12S, and 16S rRNA) and three nuclear DNAs (β-fibrinogen, IRBP, and TTR). Buckley-Beason *et al.* [61] thought that *P. uncia* was the sister taxon to the other three *Panthera* species (*P. pardus*, *P. onca*, and *P. tigris*) based on analysis of combined mtDNA (ATP8, Cyt *b*, ND5, and the control region) and nuclear gene segments (ATP-7A, BGN, HK1, IDS, and PLP). However, Jae-Heup *et al.* [41] suggested that *P. uncia* was the closest relative of *P. tigris* based on the complete mtDNA control region. *P. uncia* has also been alternatively hypothesized as the sister species of *P. tigris* based on analysis of chemical signals [14], combined nuclear DNA (combining 19 autosomal, five X-linked, and six Y-linked genes and representing 18853 bp) [1], Genomic paw prints [51] and combined dataset (the autosomes, both sex chromosomes and the mitochondrial genome and representing 47.6 kb) [62]. Our phylogenetic analyses strongly support the closest affinity between *P. uncia* and *P. leo*, which is obviously different to the relationship between the two species presented in all previous studies. In conclusion, although the precise relationships among the genus *Panthera* were not well resolved in our analyses, the combined mtDNA data, however, provided insightful understanding of the evolution of the genus *Panthera*.

3.4 Divergence time estimation

Molecular dating of the genus *Panthera* radiation had been attempted in several previous studies. Moreover, the results were slightly different based on different methods used. Discrepancies between molecular and paleontological estimates of the divergence time of the genus *Panthera* have been recently pointed out [1,15]. According to current paleontological evidences, the earliest *Panthera* fossil from the East African Pleistocene, as well as fossils of a European Pleistocene cat *Panthera gombaszoegensis*, was about 2 MYA. Early dating information based on molecular data suggested that the genus *Panthera* diverged within 1-2 MYA [54,55]. However, Janczewski *et al.*[18], using 12S rRNA and Cyt *b* sequences, made a detailed estimation of the divergence time for the Pantherine lineage and concluded that the genus *Panthera* diverged within the last 3 MYA. Bininda-Emonds *et al.*[49] thought that the extant species within the genus *Panthera* radiated between 4.2 and 2.1 MYA, based on combined phylogenetic information. On the basis of a cladistical analysis of various skeletal and anatomical characters, fossil remains, and biogeography, some scientist suggested that cats of the genus *Panthera* probably evolved within the last 5 million years or so [54]. The standpoint of Johnson *et al.*[1] was that available fossils underestimate the first occurrence by an average of 76% or 73%, and by an average of 79% for intra-*Panthera* divergence time, by analyzing autosomal, X-linked, Y-linked, and mitochondrial gene segments and 16 fossil calibrations.

The divergence times of *N. nebulosa* and the genus *Panthera* from other species of Felidae occurred at about 11.3 MYA. *N. nebulosa* was first split from other felid species, which occurred at about 8.66 MYA, with a rough range of 9.3–5.2 MYA. The divergence within the genus *Panthera* was about 10 to 1 MYA, this divergence occurred during the late Miocene and early Pliocene periods. The time of

divergence of *P. tigris* from the genus *Panthera* was 6.55 MYA, with a rough range of 6.8–2.6 MYA. The time of the split for *P. pardus* was 4.35 MYA, with a rough range of 4.6–1.82 MYA, and the time of the split for *P. uncia* was 4.63 MYA, with a rough range of 4.8–1.2 MYA. These divergence times were older than those indicated by fossil records: *P. tigris* was estimated at 1.6–1.8 MYA [54,56] and *P. pardus* was estimated at 1.3 MYA [63]. Our estimation of the divergence times of the genus *Panthera* show good agreement with other recent estimations [1,18,49].

3.5 Relationships between cladogenetic events and speciation of *P. uncia* and uplift of the Qinghai-Tibetan Plateau

The divergence time of *P. uncia*, a unique species of the Qinghai-Tibetan Plateau, was consistent with the uplift of the Qinghai-Tibetan Plateau and climate shift. Geological studies indicated that rising of the Qinghai-Tibetan Plateau was a multistage, multispeed, and heterogeneous process of in southwestern China. In particular, the tectonic events and intensive uplift that happened at about 8, 3.6, 2.5, and 1.7 MYA significantly impacted the formation of the plateau and the climate shift [64]. Molecular estimates of divergence times revealed that the major cladogenetic events of *P. uncia* occurred at these phases. At about 8 MYA, many environmental events and climatic changes happened in most areas of the Northern Hemisphere, such as enhanced upwelling in the Arabian Sea, and signified the onset or enhancement of the Indian monsoon [65]. Strong faulting of the Yangbajing Graben in northwestern Lahsa also happened during this period [66], as did the stratigraphical permanent color change and intensive arid climate development of the Linxia Basin (7.78–6.25 MYA) [67], the climate drying of the Asian inland, and the onset of both the Indian and Eastern Asian monsoons [68]. All these events indicated that intensive changes of the environment occurred on the Qinghai-Tibetan Plateau at about 8 MYA. At this time, *Panthera* originating from Asia had differentiated from the Felidae at 11.3 MYA.

The main uplift of the northwestern Qinghai-Tibetan Plateau began at 4.5 MYA [69]. The main period of salt formation was after 3.5 MYA in the Qaidam Basin. The current type of Asian monsoon began at 3.6 MYA [64, 68]. The period was named the Qinghai-Tibetan Plateau Movement A Phase [69]. *P. uncia* diverged from other species of *Panthera genus* (4.63 MYA) during this period; the primitive ancestor of *P. uncia* entered the rising Qinghai-Tibet Plateau due to some kind special or accidental opportunity and began its struggle for existence in the plateau environment. This was the first stage of the evolution of *P. uncia*.

The Asian monsoon was stably established at about 2.6 MYA, this period was named the Qinghai-Tibetan Plateau Movement B Phase [70]. Along with gradually stabilizing ecological conditions, *P. uncia* developed important morphological, behavioral, and physiological adaptations to the plateau environment in the long-term struggle for existence. This period, which was possibly the most important period for *P. uncia* evolution, was the second stage of the evolution of *P. uncia*.

The main speciation events of *P. uncia* occurred mostly after 1.7 MYA. Violent climate shift on the Qinghai-Tibetan Plateau happened at about 1.7 MYA, and the Qinghai-Tibet Plateau reached an altitude close to its current level. This period was called the Qinghai-Tibetan Plateau Movement C Phase [70]. At the same time, *P. uncia* that was distributed in the tableland radiated to the surrounding area and evolved into a Plateau endemic species. The main divergence event and radiation of *P. uncia* was corresponded well to the geological tectonic events and intensive climate shifts, implying that the evolution of *P. uncia* was in close connection with the marked environmental changes accompanied the step-by-step rising of Qinghai-Tibetan Plateau. The evolutionary process and distribution pattern *P. uncia* were direct results of their adaptation to environmental and climatic changes on the plateau.

This work was supported by grants from the National Natural Science Foundation of China (Grant Nos: 30470244 and 30870359), the Foundations for Excellent Youth in Anhui Province (Grant No: 04043409), the National Natural Science Foundation of Education Department of Anhui Province (Grant No: KJ2009B015) and the Key Laboratory of Biotic Environment and Ecological Safety in Anhui Province.

1 Johnson W E, Eizirik E, Pecon S J, *et al*. The late radiation of modern Felidae: A genetic assessment. Science, 2006, 311: 73–77
2 Werdelin L. Small pleistocene felines of North America. J Vert Paleo, 1985, 5: 194–210
3 Hunt M H J. Biogeography of the order Carnivora. In: Carnivore Behavior, Ecology, and Evolution. Vol 2. New York: Cornell University Press, 1996. 485–541
4 Werdelin L. Morphological patterns in the skulls of cats. Biol J Syst, 1983, 19: 375–391
5 Radinsky L B. Evolution of skull shape. Representative modern carnivores. Biol J Linnean Soc, 1981, 15: 369–388
6 Wurster-Hill D H, Centerwall W R. The interrelationships of chromosome banding patterns in Procyonids, Viverrids and Felids. Cytogenet Cell Genet, 1982, 34: 178–192
7 Modi W S, O'Brien S J. Quantitative cladistic analysis of chromosomal banding data among species in three orders of mammals: Hominoid primates, felids and arvicolid rodents. In: Chromosome Structure and Function. New York: Plenum, 1988. 215–242
8 Salles L O. Felid phylogenetics: extant taxa and skull morphology (Felidae Aeluroidea). American Museum Novitates, 1992, 3047: 1–67
9 Collier G E, O'Brien S J. A molecular phylogeny of the Felidae: Immunological distance. Evolution, 1985, 39: 437–487
10 O'Brien S J, Collier G E, Benveniste R E, et al. Setting the molecular clock in Felidae: the great cats Panthera. In: Tilson R L, Seal U S, editors. Tigers of the world: The biology, biopolitics, management and conservation of an endangered species. Park Ridge, New York: Noyes Publications. 1987. 10–27
11 Pecon S J, Johnson W E, Goldman D, et al. Phylogenetic reconstruction of South American felids defined by protein electrophoresis. Mol Evol, 1994, 39: 296–305
12 Benveniste R E. The contributions of retroviruses to the study of mammalian evolution. In Molecular Evolutionary Genetics. New

York: Plenum, 1985. 359–417
13 Pecon S J, O'Brien S J. Patterns of Y and X chromosome DNA sequence divergence during the Felidae radiation. Genetics, 1998, 148: 1245–1255
14 Bininda-Emonds O R. The utility of chemical signals as phylogenetic characters: an example from the felidae. Biol J Linnean Soc, 2001, 72: 1–15
15 Johnson W E, O'Brien S J. Phylogenetic reconstruction of the Felidae using 16S rRNA and NADH-5 mitochondrial genes. Mol Evol, 1997, 44: 98–116
16 Saccone C, Lanave C, Pesole G, et al. Influence of base composition on quantitative estimates of gene evolution. Methods Enzymol, 1999, 183: 570–583
17 Wu X B, Zheng T, Jiang Z G, et al. The mitochondrial genome structure of the clouded leopard (*Neofelis nebulosa*). Genome, 2007, 50: 252–257
18 Janczewski D N, Modi W S, Stephens J C, et al. Molecular evolution of mitochondrial 12S RNA and cytochrome *b* sequences in the Pantherine lineage of Felidae. Mol Biol Evol, 1995, 12: 690–707
19 Lopez J V, Cevario S, O'Brien S J. Complete nucleotide sequences of the Domestic cat (*Felis catus*) mitochondrial genome and a transposed mtDNA tandem repeat (Numt) in the nuclear genome. Genomics, 1996, 33: 229–246
20 Burger P A, Steinborn R, Walzer C, et al. Analysis of the mitochondrial genome of cheetahs (*Acinonyx jubatus*) with neurodegenerative disease. Gene, 2004, 338:111–119
21 Rychlik W, Rychlik P. Oligo Primer Analysis Software. Version6.01. Molecular Biology Insights, Inc., Cascade, Colorado. 2000
22 Altschul S F, Madden T L, Schäer A A, et al. Gapped BLAST and PSI-BLAST: a new generation of protein database search programs. Nucleic Acids Res, 1997, 25: 3389–3402
23 Thompson J D, Gibson T J, Plewniak F, et al. The clustal X windows interface: flexible strategies for multiple sequence alignment aided by quality analysis tools. Nucleic Acids Res, 1997, 25(24): 4876–4882
24 Swofford D L. PAUP*: Phylogenetic Analysis Using Parsimony (and Other Methods). 2003
25 Huelsenbeck J P, Hillis D M. Success of phylogenetic methods in the four-taxon case. Syst Biol, 1993, 42: 247–264
26 Ronquist F, Huelsenbeck J P. MrBayes 3: Bayesian phylogenetic inference under mixed models. Bioinformatics, 2003, 19: 1572–1574
27 Posada D, Buckley T R. Model selection and model averaging in phylogenetics: advantages of the AIC and Bayesian approaches over likelihood ratio tests. Syst Biol, 2004, 53: 793–808
28 Rannala B, Yang Z. Probability distribution of molecular evolution trees: a new method of phylogenetic inference. Mol Evol, 1996, 43:304–311
29 Leache´ A D, Reeder T W. Molecular systematics of the eastern fence lizard (*Sceloporus undulatus*): a comparison of parsimony, likelihood, and Bayesian approaches. Syst Biol, 2002, 51: 44–68
30 Shimodaira H, Hasegawa M. Multiple comparisons of log-likelihoods with applications to phylogenetic inference. Mol Biol Evol, 1999, 16: 1114–1116
31 Asakawa S, Kumazawa Y, Araki T, et al. Strand-specific nucleotide composition bias in echinoderm and vertebrate mitochondrial genomes. Mol Evol, 1991, 32: 511–520
32 Arnason U, Gullberg A, Gretarsdottir S, et al. The mitochondrial genome of the sperm whale and a new molecular reference for estimating eutherian divergence dates. Mol Evol, 2000, 50: 569–578
33 Hillis D M, Moritz C. An overview of applications of molecular systematics. Molecular Systematics. Sinauer Associates, Sunderland, Ma. 1990
34 Glazko G V, Nei M. Estimation of divergence times for major lineages of primate species. Mol Biol Evol, 2003, 20: 424–434
35 Yang Z, Yoder A D. Comparison of likelihood and Bayesian methods for estimating divergence time using multiple gene loci and calibration points, with application to a radiation of cute-looking mouse lemur species. Syst Biol, 2003, 52: 705–716
36 Waddell P J, Cao Y, Hasegawa M, et al. Assessing the Cretaceous superordinal divergence times within birds and placental mammals by using whole mitochondrial protein sequences and an extended statistical framework. Syst Biol, 1999, 48: 119–137
37 Nilsson A M, Gullberg A, Spencer P, et al. Marsupial relationships and a timeline for marsupial radiation in South Gondwana. Gene, 2004, 340: 189–196
38 Huelsenbeck J P, Rannala B. Phylogenetic methods come of age: Testing hypotheses in an evolutionary context. Science, 1997, 276: 227–232
39 Janke A, Arnason U. The complete mitochondrial genome of Alligator mississippiensis and the separation between recent archosauria (birds and crocodiles). Mol Biol Evol, 1997, 14: 1266–1272
40 Kumar S, Tamura K, Nei M. MEGA3: Integrated software for molecular evolutionary genetics analysis and sequence alignment. Brief Bioinform, 2004, 5: 150–163
41 Jae-Heup K, Eizirik E, O'Brien S J, et al. Structure and patterns of sequence variation in the mitochondrial DNA control region of the great cats. Mitochondrion, 2001, 3: 279–292
42 Sun Y, Ma F, Xiao B, et al. The complete mitochondrial genomes sequences of *Asio flammeus* and *Asio otus* and comparative analysis. Sci China Ser-C Life Sci, 2004, 47: 510–520
43 Xu X, Gullberg A, Arnason U. The complete mitochondrial DNA (mtDNA) of the donkey and mtDNA comparisons among four closely related mammalian species-pairs. Mol Evol, 1996, 43: 438–446
44 Kim K S, Seong E L, Ho W J, et al. The complete nucleotide sequence of the domestic dog (*Canis familiaris*) mitochondrial genome. Mol Phylogenet Evol, 1998, 10: 210–220
45 Gissi C, Gullberg A, Arnason U. The Complete mitochondrial DNA sequence of the Rabbit (*Oryctolagus cuniculus*). Genomics, 1998, 50: 161–169
46 Sano N, Kurabayashi A, Fujii T, et al. Complete nucleotide sequence and gene rearrangement of the mitochondrial genome of the bell-ring frog, *Buergeria buergeri* (family Rhacophoridae). Genes Genet Syst, 2004, 79: 151–163
47 Han D M, Zhou K Y. Complete sequence and gene organization of the mitochondrial genome of Tokay (*Gekko gecko*). Zool Res, 2005, 26: 123–128
48 Frazer-Abel A A, Hagerman P J. Determination of the angle between the acceptor and anticodon stems of a truncated mitochondrial tRNA. Mol Biol, 1999, 85: 581–593
49 Bininda-Emonds O R, Gittleman J L, Purvis A. Building large trees by combining phylogenetic information: a complete phylogeny of the extant Carnivora (Mammalia). Biol Rev, 1999, 74: 143–175
50 King V, Goodfellow P N, Pearks W A J, et al. Evolution of the male-determining gene SRY within the cat family Felidae. Genetics, 2007, 175: 1855–1867
51 O'Brien S J, Johnson W E. The evolution of cats. Genomic paw prints in the DNA of the world's wild cats have clarified the cat family tree and uncovered several remarkable migrations in their past. Sci Am, 2007, 297: 68–75
52 Yu L, Li Q W, Ryder O A, et al. Phylogenetic relationships within mammalian order Carnivora indicated by sequences of two nuclear DNA genes. Mol Phylogenet Evol, 2004, 33: 694–705
53 Kurten B, Anderson E. Pleistocene mammals of North America. New York: Columbia University Pree, 1980
54 Wayne R K, Benveniste R E, Janczewski D N, et al. Molecular and biochemical evolution of the Carnivora. In Carnivore Behaviour, Ecology and Evolution, London: Chapman and Hall, 1989. 465–494
55 Neff N A. The Big Cats: The Painting of Guy Coheleach. New York: Abrams, 1982
56 Hemmer H. The evolutionary systematics of living Felidae: present status and current problems. Carnivore, 1978, 1: 71–79
57 Pocock R I. Notes upon some African species of the genus Felis, based upon specimens recently exhibited in the society's garden. Proc Zool Soc Lond, 1907, 77: 656–667
58 Yu L, Zhang Y P. Phylogenetic studies of pantherine cats (Felidae) based on multiple genes, with novel application of nuclear β-fibrinogen intron 7 to carnivores. Mol Phyl Evol, 2005, 35: 483–495
59 Pecon S J, Wilkerson A J P, Murphy W J, et al. Phylogenetic Assessment of Introns and SINES within the Y chromosome using the

cat family Felidae as a species tree. Mol Biol Evol, 2004, 21: 2299–2309
60 Mattern M Y, McLennan D A. Phylogeny and speciation of Felids. Cladistics, 2000, 16: 232–253
61 Buckley-Beason V A, Johnson W E, Nash W G, et al. Molecular evidence for species-level distinctions in clouded leopards. Curr Biol, 2006, 16: 2371–2376
62 Davis B W, Li G, Murphy W J. Supermatrix and species tree methods resolve phylogenetic relationships within the big cats, Panthera (Carnivora: Felidae). Mol Phylogenet Evol, 2010, 56: 64–76
63 Turner A. New fossil carnivore remains from the Sterkfontein hominid site (Mammalia: Carnivora). Ann Transvall Mus, 1987, 34: 319–347
64 Li J J, Fang X M, Pan B T. Late Cenozoic intensive uplift of Qinghai-Xijiang Plateau and its impacts on environments in surrounding area. Quat Sci, 2001, 21: 381–391
65 Kroon D, Steen T, Troelstra S R. Onset of monsoonal related upwelling in the western Arabian Sea as revealed by planktonic foraminifers. Proc Ocean Drill Prog Sci Res, 1991, 117: 257–263
66 Harrison T M, Copeland P, Kidd W S F, et al. Activation of the Nyainqentanghla shear Zone: Implications for uplift of the southern Tibetan Plateau. Tectonics, 1995, 14: 658–676
67 Dong M, Fang X M, Shi Z T, et al. The absolute age and division of Cenozoic stratum from the Linxia Basinin Gansu province, Chinese Science Bulletin (in Chinese), 1997, 14: 1458–1471
68 An Z, Kutzbach J E, Prell W L, et al. Evolution of Asian monsoons and phased uplift of the Qinghai-Tibetan Plateau since late Miocene times. Nature, 2001, 411: 62–66
69 Zheng H, Powell C M, An Z, et al. Pliocene uplift of the northern Tibet plateau. Geology, 2000, 28: 715–718
70 Li J J, Fang X M, Ma H Z, et al. Geomorphologic and environmental evolution in upper reaches of Yellow River during the late Cenozoic. Sci China Ser-D Earth Sci, 1996, 39: 380–390
71 Arnason U, Adegoke J A, Bodin K, et al. Mammalian mitogenomic relationships and the root of the eutherian tree. Proc Natl Acad Sci USA, 2002, 99: 8151–8156
72 Xu X, Arnason U. The complete mitochondrial DNA sequence of the horse, Equus caballus: extensive heteroplasmy of the control region. Gene, 1994, 148: 357–362
73 Xu X, Arnason U. The complete mitochondrial DNA sequence of the white rhinoceros, Ceratotherium simum, and comparison with the mtDNA sequence of the Indian rhinoceros, Rhinoceros unicornis. Mol Phylogenet Evol, 1997, 7: 189–194
74 Xu X, Janke A, Arnason U. The complete mitochondrial DNA sequence of the greater Indian rhinoceros, Rhinoceros unicornis, and the Phylogenetic relationship among Carnivora, Perissodactyla, and Artiodactyla (+ Cetacea). Mol Biol Evol, 1996, 13: 1167–1173
75 Janke A, Feldmaier-Fuchs G, Thomas W K, et al. The marsupial mitochondrial genome and the evolution of placental mammals. Genetics, 1994, 137: 243–256
76 Desjardins P, Morais R. Sequence and gene organization of the chicken mitochondrial genome. A novel gene order in higher vertebrates. J Mol Biol, 1990, 212: 599–634
77 Johnson K P, Sorenson M D. Comparing molecular evolution in two mitochondrial protein coding genes (cytochrome b and ND2) in the dabbling ducks (Tribe: Anatini). Mol Phylogenet Evol, 1998, 10: 82–94
78 Härlid A, Janke A, Árnason Ú. The complete mitochondrial genome of Rhea americana and early avian divergences. J Mol Evol, 1998, 46: 669–679
79 Härlid A, Janke A, Árnason Ú. The mtDNA Sequence of the ostrich and the divergence between paleognathous and neognathous birds. J Mol Evol, 1997, 14: 754–761
80 Janke A, Arnason U. The complete mitochondrial genome of Alligator mississippiensis and the separation between recent Archo-sauria (birds and crocodiles). Mol Biol Evol, 1997, 14: 1266–1272
81 Wu X B, Wang Y Q, Zhou K Y, et al. Complete mitochondrial DNA sequence of Chinese alligator, Alligator sinensis, and phylogeny of crocodiles. Chinese Sci Bull, 2003, 48: 2050–2054